


INTEGRATED GEOPHYSICAL INVESTIGATION OF RIVER OGUN FLOODPLAIN, PAPALANTO, SOUTHWESTERN NIGERIA

Olumayowa Temitope IJALEYE¹ , Michael Adeyinka OLADUNJOYE², Afolabi Treasure ADEFEHINT²

¹ Department of Geology, Kogi State University, Anyigba, Nigeria

² Department of Geology, University of Ibadan, Ibadan, Nigeria

E-mail: mayaajala@yahoo.com

ABSTRACT

A geophysical investigation that involves the integration of Vertical Electrical Sounding (VES), Electrical Resistivity Imaging (ERI), and Ground Penetrating Radar (GPR) methods was conducted on Papalanto, Ogun River floodplain, a location underlain by sedimentary terrain of Southwestern Nigeria. This research aimed to image the underground lithological units and delineate the shallow geologic structures in order to characterize the area for agricultural suitability throughout the dry season. VES results typically outlined three geologic layers which are topsoil, saturated loamy clay, and alluvium. From 2D inverted resistivity results, three major geologic layers, namely topsoil, saturated loamy clay, and alluvium, were outlined and are in very good agreement with the results attained through VES. The first three layers of 3D inverted resistivity sections display a great amount of variation in the distribution of resistivity at superficial depth, made up of low resistive content. From the GPR survey, three geologic layers were also outlined from the results, namely the topsoil, saturated loamy clay, and alluvium. Consequently, the study location can be said to be semi-competent to competent luxuriant farming land in consideration of the resistivity distribution of the floodplain subsurface. Therefore, VES, ERI, and GPR are very effective geophysical methods for describing and classifying the shallow subsurface in reference to the measured physical properties. Hence, they should be applied in related geophysical investigations for better insight into the geology of the subsurface.

Keywords: Agricultural suitability; Dry season; Floodplain; Geophysical investigation; Underground lithological units.

1 INTRODUCTION

Floodplains have shallow water tables and consist of nutrient-rich silt and sediments distributed across a very wide area by floods. This makes them luxuriant lands for growing crops, especially in the dry season. They are usually not undulating with little or no boulders that may hinder farming activities. They can support particularly rich ecosystems, both in quantity and diversity [1]. When the soil of floodplains becomes wet, a gush of nutrients is released instantly which includes the remnant from the preceding flood and those resulting from the speedy breakdown of organic matter that has amassed ever since. The nutrient production fluctuates rapidly, nonetheless the gush of new sprouting plants lasts for a while, making the floodplains valued in agriculture. The physical properties of soil, namely effective depth, texture, and soil structure, are essential factors in determining soil suitability for large-sized production of crops [2]. Information about the variability of moisture content of the soil with depth and determination of rooting depth will afford a broad understanding of the struggle for soil water amid annual and cash crops. An important part is played by roots in the development of plants and is responsible for numerous roles, namely absorption of water by plant-soil, absorption of nutrient, organic matter source, storage, synthesis of growth substances, etc. [3]. Therefore, water accessibility at the right effective depth for good plant development is of a high significance to the farming scheme. Consequently, so as to guarantee an appropriate supply of water for crops growing on a floodplain that is cultivated, information about the moisture content of the soil as well as observation of its changes is of important. A geophysical method that is non-destructive for

observing the dynamics of soil water from the surface to the right depth and further on without disturbing the soil is provided by Electrical resistivity method. Electrical resistivity has close relationship with the quantity of water available in the soil. The resistivity of soil is dependent on the amount of saturation, permeability, ionic concentration of the fluids in the pore, and clay content [5]. It is therefore one of the geophysical methods mostly applied to identify changes in moisture content of the soil, flow pattern of groundwater, and depth to water-saturated zone [6]. Numerous geophysical methods have been made use of in studying the infiltration of soil water. The geo-electrical resistivity method is among the geophysical methods that can be employed to map and characterize spatial and temporal variations in the physical properties of soil [7, 8]. The electrical resistivity method is found to be inexpensive, fast, and dependable for stress-free prediction of soil physical properties [9]. Significant variations in the electrical conductivity of the soil can be caused by rainfall, periodic changes in temperature of the soil, salinity, porosity, the structure of the soil, air voids, and changes in water content of soil [9, 10]. Electrical Resistivity survey, particularly 2D Electrical Resistivity Tomography (ERT), have been used by numerous scholars for the purpose of agriculture [11, 12]. The connection between electrical resistivity of soil and moisture content have been determined with the use of soil analysis [13, 14], while margins of soil horizons were identified and bedrocks at different degree of weathering process were detected using GPR and VES methods respectively [15]. Vertical electrical sounding (VES) and 2D electrical resistivity tomography (ERT) are geo-electrical methods applied to the understanding of subsurface lithology and to define groundwater potential zones [16, 17]. In addition, observation of content of soil water have been carried out by many researchers with the use of 2D ERT or VES geophysical methods [18, 19]. Ground Penetrating Radar (GPR) and electrical resistivity techniques have abundant benefits over conventional soil and sediment investigation techniques such as pits, cores, or trenches. GPR affords highly defined and uninterrupted profiles of the subsurface when correctly used while resistivity provides facts about the layers of the earth. This makes available a much larger quantity of information than taking samples separately through coring or digging [20–22]. In cases where excavation is required, GPR in addition to electrical resistivity methods can be beneficial in the coring sites selection, making the best use of effort in areas of curiosity or indecision [23]. The non-destructive nature of GPR can be appreciated in research locations that are sensitive, for example archeological sites or ecological areas that are protected. Also, electrical resistivity method is found appropriate for exploration of groundwater, mineral exploration, archaeological sites and geo-techniques investigations. In general, GPR and electrical resistivity methods are very effective in giving researchers the ability to image the subsurface [24].

The objectives of the current study includes the integrated application of VES and ERI to observe of soil water content variation with depth within the floodplain subsurface, to determine the actual depth that can sustain the floodplain farming particularly in dry season, determination of the groundwater level, to map the shallow water table depth and identification of soil horizons in the floodplain subsurface with the use GPR method. Furthermore, the study also aims at determination of the geo-electrical layers and geo-electrical parameters within the floodplain with the use of Vertical Electrical Sounding (VES) results.

2 SITE DESCRIPTION AND GEOLOGICAL SETTING

The study location is the floodplain of River Ogun situated in Papalanto town in the Ewekoro Local Government Area of Ogun State, South-western part of Nigeria (Fig.1). It is positioned between longitudes N06°51'57.2"–N06°52'02.0" and latitudes E003°14'05.1"–E003°14'06.2" covering an area of around 22.5km². The topography of the study location is almost flat and generally rock outcrops are absent. The elevation ranges from 17 to 25 m and is drained by the Ogun River. The network of the drainage system of this region is high and typical of several big perennial rivers, such as Ogun, Ewekoro, and Berre, which frequently have dendritic drainage patterns [25]. This drainage pattern can be distinguished by the uneven splitting of rivers with flow direction naturally in the north direction. The area studied is situated in the humid tropical rain forest region of Nigeria which is typical of two climatic seasons, namely the rainy season and the dry season, which last for about eight months (March–October) and four months (November–February) respectively. It has an average yearly rainfall of 1300 mm, and potential evapotranspiration of nearly 188 mm.

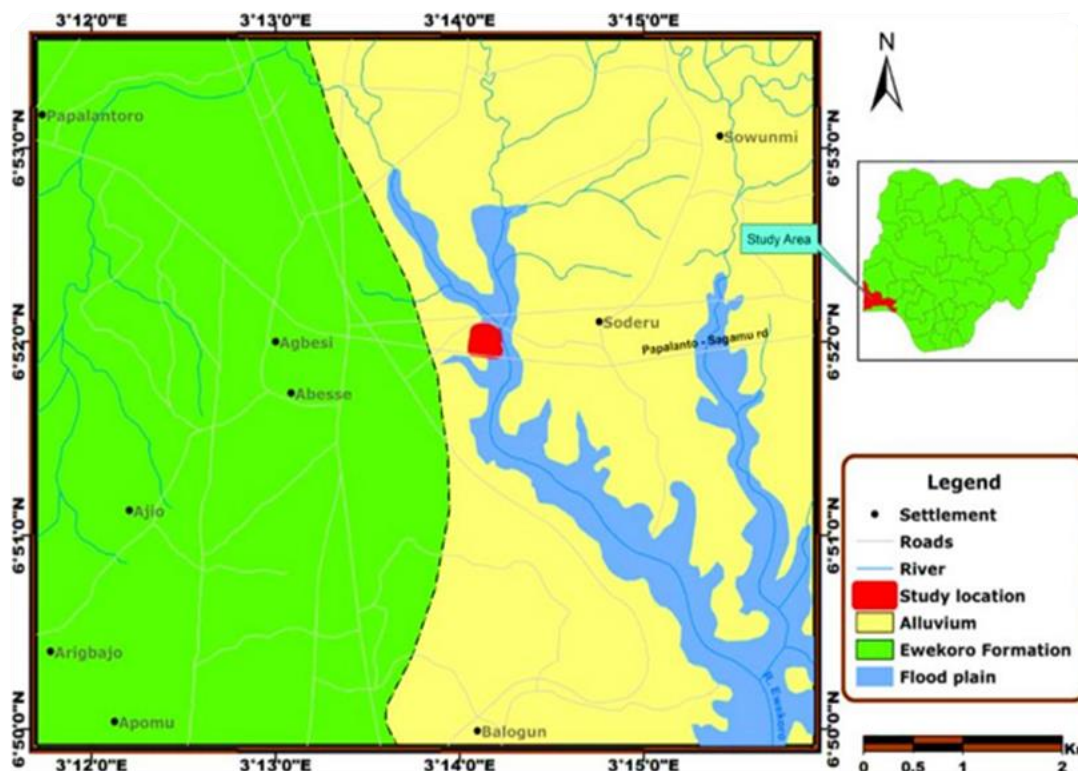


Figure 1. Location Map of Papalanto, River Ogun Floodplain, Inset: Map of Nigeria [26]

2.1 Geology of the study area

The study location is in the sedimentary basin. It occupies a portion of the Abeokuta group of the Dahomey Basin. Dahomey Basin extends through south-eastern Ghana through Togo and the Benin Republic to the western margin of the Nigerian Niger Delta. The Abeokuta group is made up of sandstone which is coarse-grained, poorly sorted, micaceous, and ferruginous. This sandstone is arkosic with fair to good bedding. Intercalation of marine shale and mudstone negligibly present [27]. The basal members of the formation are of an unknown age. It is undoubtedly diachronous and is possibly not older than Maastrichtian (Fig. 3). The Abeokuta Group in addition to Ewekoro Formation, Coastal Plain Sands, and recent sediments create diverse aquifers in the Dahomey Basin on which Papalanto is accommodated. The aquifer can be categorized into confined, semi-confined, and unconfined subject to the type of the aquifer units and the adjacent layers of rock [28]. The sands of the coastal plain and sediment aquifers that are recent are unconfined aquifers found at shallow depth. They are predisposed to contamination from ground sources and run-off water and have changing depths with topography and seasons. Semi-confined aquifers exist in Ilaro formation because of the irregular sequence of sand and clay stratigraphy. Where the sand unit is bounded at the top and bottom by the low-permeable clay layers, the aquifers are confined. At superficial depth, the marine sand aquifers are not confined but have brackish water constituents. In the Ewekoro formation, the aquifer is limestone, while continental sands constitute the aquifer in Abeokuta formation (Fig. 2).

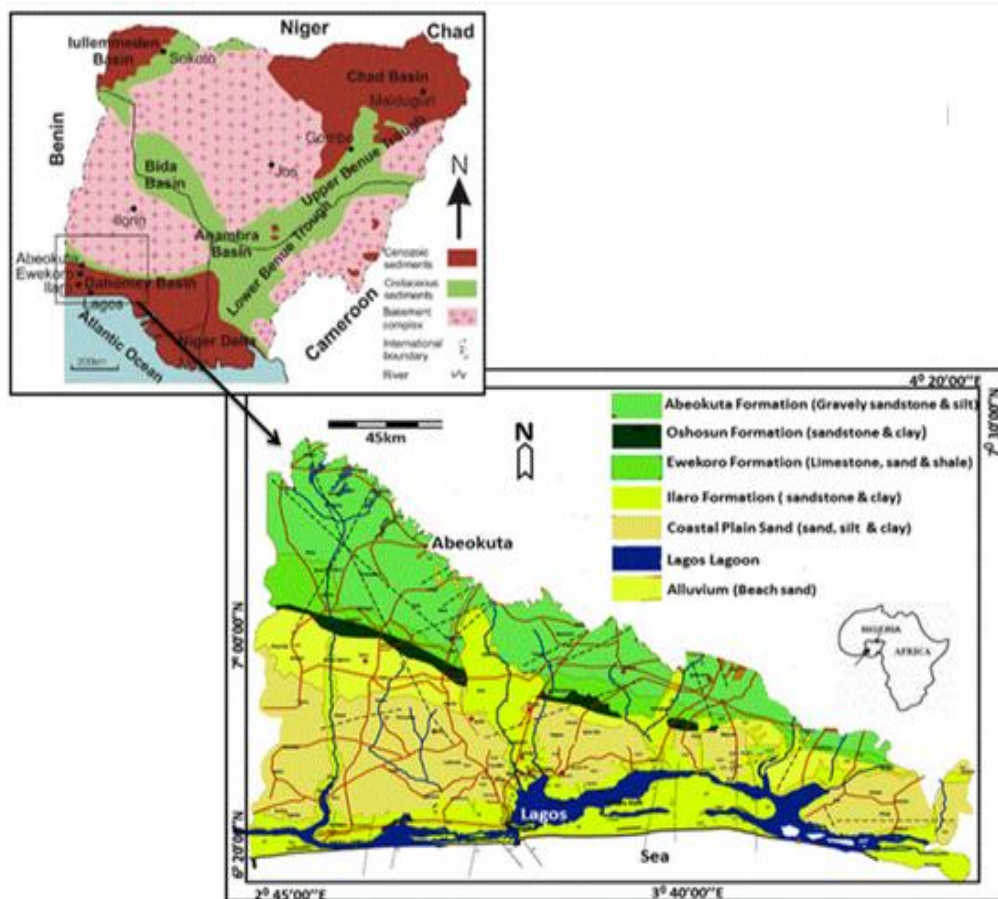


Figure 2. Aquifer map of the Dahomey Basin showing the limestone and continental sands constituents of the aquifer in Ewekoro and Abeokuta Formation respectively in Nigeria, Inset: Map of Nigeria [29]

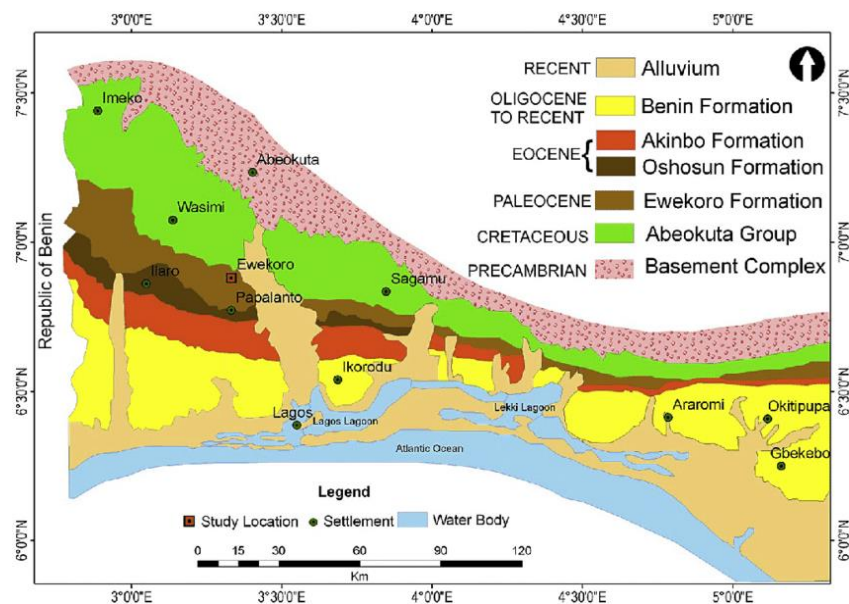


Figure 3. The map of geology of eastern Dahomey Basin (Nigerian portion) showing the study location [30]

3 METHODOLOGY

3.1 Reconnaissance survey

Careful reconnaissance mapping is crucial in the planning and designing of any geophysical survey. The floodplain was visited to map its area extent and to determine the suitability of the site for this research. The visitation allows us to examine site characteristics, such as land cover, topographic information, floodplain characteristics, and the sediment accumulated over time. It also helps to determine the saturation state of the site in order to have a proper plan for data acquisition and to spatially distribute the profile lines on it.

3.2 Geological investigation

Geological investigation of the study location was conducted to find out the geology, that is the rock types, of the study location. The tools used for this investigation are Base map, Global Positioning System (GPS), Compass clinometer, and field notebook.

3.3 Geophysical investigation

An integrated geophysical investigation which comprises of the Electrical Resistivity methods (Electrical Resistivity Imaging (ERI) and Vertical Electrical Sounding (VES)) and Ground Penetrating Radar (GPR) survey was conducted in the study area (Fig. 4).

3.3.1 Electrical Resistivity Methods

Electrical resistivity survey is highly effective since electrical resistivity is a factor that can illustrate the heterogeneity of a geological medium, taking cognizance of lithological and hydrological aspects of it [31, 32]. The variation in electrical properties of sub-surface materials makes the resistivity technique a very good method in sub-surface characterization. The disparity in lithological sequence, water saturation, fluid conductivity, permeability, and porosity usually associate with the variability in electrical resistivity (conductivity) in which inferences about geological structure, groundwater potential, fractures/fault zone, sinkhole, and stratigraphic units can be drawn from it. For this research, Electrical Resistivity Imaging (ERI) and Vertical Electrical Sounding (VES) were adopted. The survey was carried out with the electrical current injected into the sub-surface using two electrodes (current electrodes), while the geological medium serves as a resistor. The drop-in voltage is recorded using the two different electrodes (potential electrodes) and is directly proportional to the electrical resistance of the medium. The measurement recorded in the field is known as apparent resistivity.

The ERI was carried out by implanting electrodes along the profile but only four were made use of at each measurement. The measurement was achieved by manually shifting the electrodes along the profile line with the least electrode spacing of 5 m and the apparent resistivity obtained. For each level, the minimum electrode spacing was used for data acquisition, and once completed; the electrode spacing is increased by the addition of minimum electrode spacing to the last electrode spacing until the number of levels has been achieved. Pseudosection and contour were generated from the apparent resistivity value obtained for each measurement. Ten ERI profiles were spatially distributed on the study site with profiles 1 to 5 occupying the North-South direction, while profiles 6 to 10 were oriented in the West-East direction. Wenner electrode arrangement was adopted for this research with a minimum electrode spacing of 5 m, and 30 m was the maximum electrode spacing which is the last electrode spacing for each profile. The 2D ERI data obtained for each profile line were combined into a gridded 3D view of the inverted resistivity model. The 2D profiles were arranged parallel to each other in the X and Y directions. The 2D data were converted using RES2Dinv commercial software into the 2D model of the subsurface which is presented in model blocks [33]. A sharp and straight boundary of the separate different layers with variable resistivity values was obtained using the robust data constraint option [34]. For the collated 3D data set, RES3Dinv commercial software was used for its inversion to produce a depth slice which allows for the identification of different anomalies in space and depth. The VES data was obtained using Schlumberger electrode arrangement

with half electrode 180 separation ($AB/2$) ranges from 100 m to 133 m. The distance between the collinearly arranged potential electrodes is kept constant, while that of the spacing of the current electrodes changes for each measurement. The potential electrode spacing can only change when the observed potential across the current electrodes is too small. The 2D ERT and VES data were acquired using Campus Tigre resistivity meter with error observed during the acquisition less than 1%. The VES data plotted on a bi-logarithm graph and the curves were matched with appropriate theoretical curves. The model parameter generated from the initial curve matching was used as initial parameters for data inversion using WinRESIST.

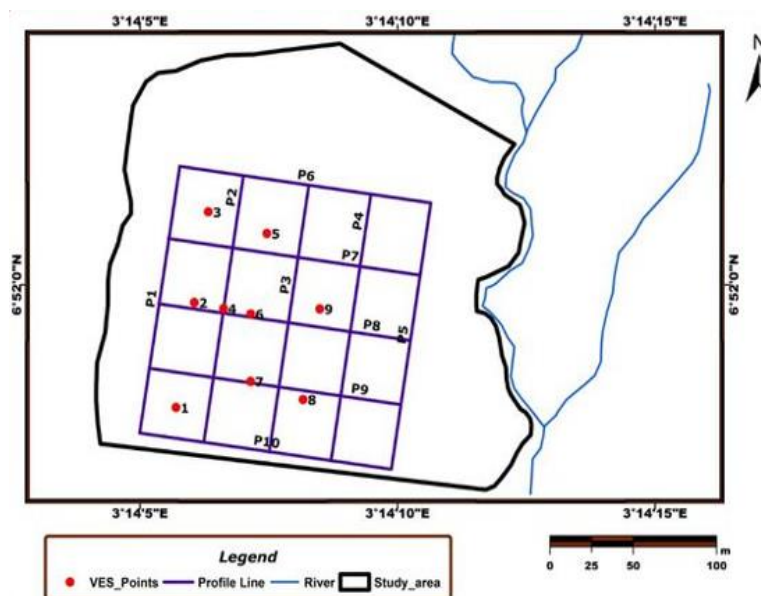


Figure 4. Map showing VES and ERI distribution points and GPR lines

3.3.2 Ground Penetrating Radar

The success of any ground penetrating radar (GPR) survey depends on the proper design of the survey. A total of ten (10) GPR profile lines of 150 m in length were acquired and labelled (P1 to P10). Profiles 1 to 5 were acquired in the north-south direction, while profiles 6 to 10 were acquired in the west-east direction (Fig. 4). The profiles were established with the help of measuring tape and handheld Garmin GPS. The inter profile spacing used for the acquisition was 37.5 m to give equal distribution across the study area. SIR system-3000 GPR equipment with a 400MHz frequency antenna was used to provide good quality data and sufficient depth of penetration for the intended research work. The GPR system was wheeled in a cart with an odometer and it was set at 2cm trace spacing with auto stack mode. The sampling frequency was set at 4030MHz which was adjudged to be adequate for this investigation alongside a sampling window of 120 nano seconds (ns). The system was set at 64 scans per second and 25 scans per meter with a point gain of 5. The dielectric constants of 16 with 100 MHz vertical high pass filter and 800 MHz vertical low pass filter were used.

The data was transferred from the GPR equipment to RADAN-7, a 2D & 3D Software for GPR data processing & interpretation. The standard steps for GPR data filtering processes were adopted to have a good radar signal presented for interpretation. The data was subjected to a dewow to remove low frequency component from it and the ringing effect was reduced by removing the background noise. Noises associated with frequencies in contrast with the signal was reduced by using a band pass filter. This aids the removal of unwanted noises at high and low ends of the amplitude spectrum [35, 36]. To improve the quality of the radar image, the gain function was manually adjusted and the total time window was trimmed to 90 ns. The processed radar section was visually inspected to preliminary identified anomalous spots which were later followed by quantitative characterization by attribute analysis. The processed radar sections were interpreted based on the principles of radar stratigraphy which was adopted from seismic stratigraphy [37].

4 RESULTS AND DISCUSSION

4.1 Vertical Electrical Sounding (VES) Results

The results of the VES inversion present geoelectric layer parameters in the form of layer resistivity and thickness which were used to characterize the subsurface in the study area. VES curves typical of the investigated area are presented in Fig. 5. The sounding curves acquired in the investigated area are three layers which are H type. The layers obtained from the sounding curves from top to bottom for the study area include: topsoil which is made up of organic matter and peat, saturated loamy clay formation, and alluvium. The topsoil and saturated loamy clay are characterized by low resistivity values so much more that they can easily be ignored and interpreted as a single layer. The presence of clay materials within these first two layers caused the decrease in their resistivity value and it also help these layers to accumulate and retain water due to its characteristics of high porosity, low specific yield and low permeability [38]. This clay character of high porosity, low specific yield and low permeability enhanced the storage of water within these layers for a long period of time, which supports dry season farming on the floodplain. The VES results were summarized, interpreted and presented in Table 1. The variations in different geoelectric layers for the study area are shown in Fig. 6, which helps to understand the kind of material that constitute each layer from the top to the bottom. The resistivity of the topsoil varies from 8 Ωm to 134 Ωm with average resistivity value of 53 Ωm . The topsoil has an average thickness of about 1.4 m. The observed variation was as a result of different materials that formed the topsoil around the study area. Based on the field and resistivity data observation, the topsoil is composed of organic matter, organic peat and sandy loamy in some areas. The organic matter and peat gave it the dark colouration observed during the field work. The saturated loamy clay has resistivity value ranging from 3 Ωm to 9 Ωm , with average resistivity of 5 Ωm . This layer is made up of virtually the same material component across the study area due to non-copious variation in values of resistivity obtained. Observation from the acquired resistivity data indicated that this layer was saturated and was made up of admixture of clay and loamy soil with a high proportion of clay present. The material compositions of this layer have high water retention capacity which yields its water for food crop farming during dry season in this floodplain. Clay has a very notable characteristic of being dense and also all available pores that can easily be drained within the soil particles are either temporarily or permanently filled with water which made it slick when touched. Clay soil can hold both moisture and nutrients due to its density. These characteristics of the first two layers identified with the study area aid dry season farming within the floodplain. These two layers are also being replenished constantly due to recurrent floods along the floodplain which give good agricultural yield. The alluvium is the last layer captured during sounding and it has resistivity value ranging from 40 Ωm to 190 Ωm .

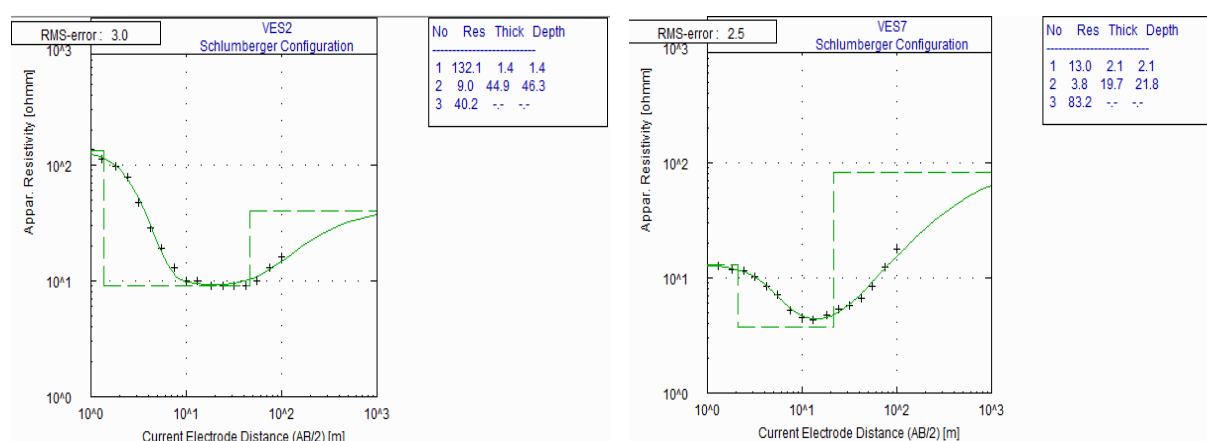
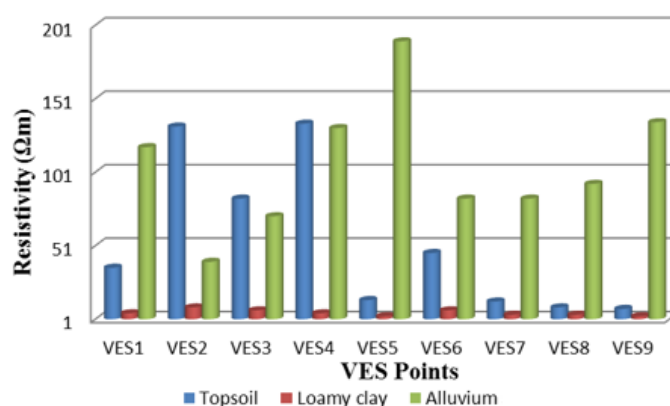


Figure 5. Representative layer model interpretation for H – curve type for Papalanto floodplain VES

Table 1. Summarized VES results and interpretation for the studied area

VES No	Resistivity (ρ) (Ωm)	Thickness (h) (m)	Depth	Curve Type	Lithology
1	36/5/118	1.3/29.6	1.3/30.9	H	Topsoil / Saturated loamy clay / Alluvium
2	132/9/40	1.4/44.9	1.4/46.3	H	Topsoil / Saturated loamy clay / Alluvium
3	83/7/71	1.6/38.2	1.6/39.8	H	Topsoil / Saturated loamy clay / Alluvium
4	134/5/131	1.8/31.8	1.8/33.6	H	Topsoil / Saturated loamy clay / Alluvium
5	14/3/190	1.3/16.5	1.3/17.8	H	Topsoil / Saturated loamy clay / Alluvium
6	46/7/83	1.8/26.4	1.8/28.2	H	Topsoil / Saturated loamy clay / Alluvium
7	13/4/83	2.1/19.7	2.1/21.8	H	Topsoil / Saturated loamy clay / Alluvium
8	9/4/93	0.6/12.2	0.6/12.8	H	Topsoil / Saturated loamy clay / Alluvium
9	8/3/135	0.7/11.3	0.7/12.0	H	Topsoil / Saturated loamy clay / Alluvium

*Figure 6. Showing the variation of resistivity in different geoelectric layers for the study area*

4.2 Electrical Resistivity Imaging (ERI) Results

The generated 2D resistivity image from the inversion of the field data for each profile produces variability of ground resistivity from the topsoil to depth of about 18 m. Different layering and resistivity distribution were observed on all the 2D models generated which is an indication of heterogeneity of the subsurface layers around the study area. Sections produced from the 2D inverse model allow for the identification of varying true electrical resistivity of subsurface with depth along the profiles. The study is divided into north-south and west-east directions which were run perpendicular to one another in the investigated area. The north-south profiles run parallel to the river channel, including profiles 1 to 5, while the west-east profiles run perpendicular to the river channel, profiles 6–10.

The north-south directions with five profiles (Fig. 7a) and the west-east directions with five profiles (Fig. 7b) present variation in the resistivity contours whose values mostly increase from less than 5 Ωm to above 50 Ωm . These sections present the inhomogeneous nature of the subsurface which is an indication of variability of the material composition of the earth layer. All the 2D resistivity models displayed three layers as observed from the resistivity value obtained and the layers revealed are the saturated topsoil composed of loamy clay, organic matter and peat, the saturated clayey layer and saturated alluvium which sometimes occur as pocket or as an intrusion. The saturated topsoil which is made up of loamy clay, organic matter and organic peat is characterized with resistivity value of less than 2 Ωm to about 10 Ωm and is saturated. This layer occurs at the top of each profile except for profiles 1, 2, 8, 9 and 10, where there is pocket of alluvium at the surface and this was observed during

data acquisition. The observed second layer on the inverted model is the saturated clayey layer with resistivity value of $10\ \Omega\text{m}$ to about $30\ \Omega\text{m}$ [39, 40]. This layer was observed to vary in thickness across the length of the profiles and its resistivity value is sometimes not differentiated from overlying layer and thereby presenting a picture of uniform layer for the top and second layer on the inverted section. The layer revealed relatively high resistivity of above $40\ \Omega\text{m}$, which is an indication of saturated alluvium occurring as a pocket at different depths across the inverted sections. Also observed on the inverted sections was the shallow water table which was responsible for the saturation in the area. The presence of the clayey formation within the subsurface here helps to retain much water from which food crops planted in the study area draw water for circulation of nutrient, while the loamy clay soil composed of organic matter supplies the necessary nutrients for the plants during the dry season.

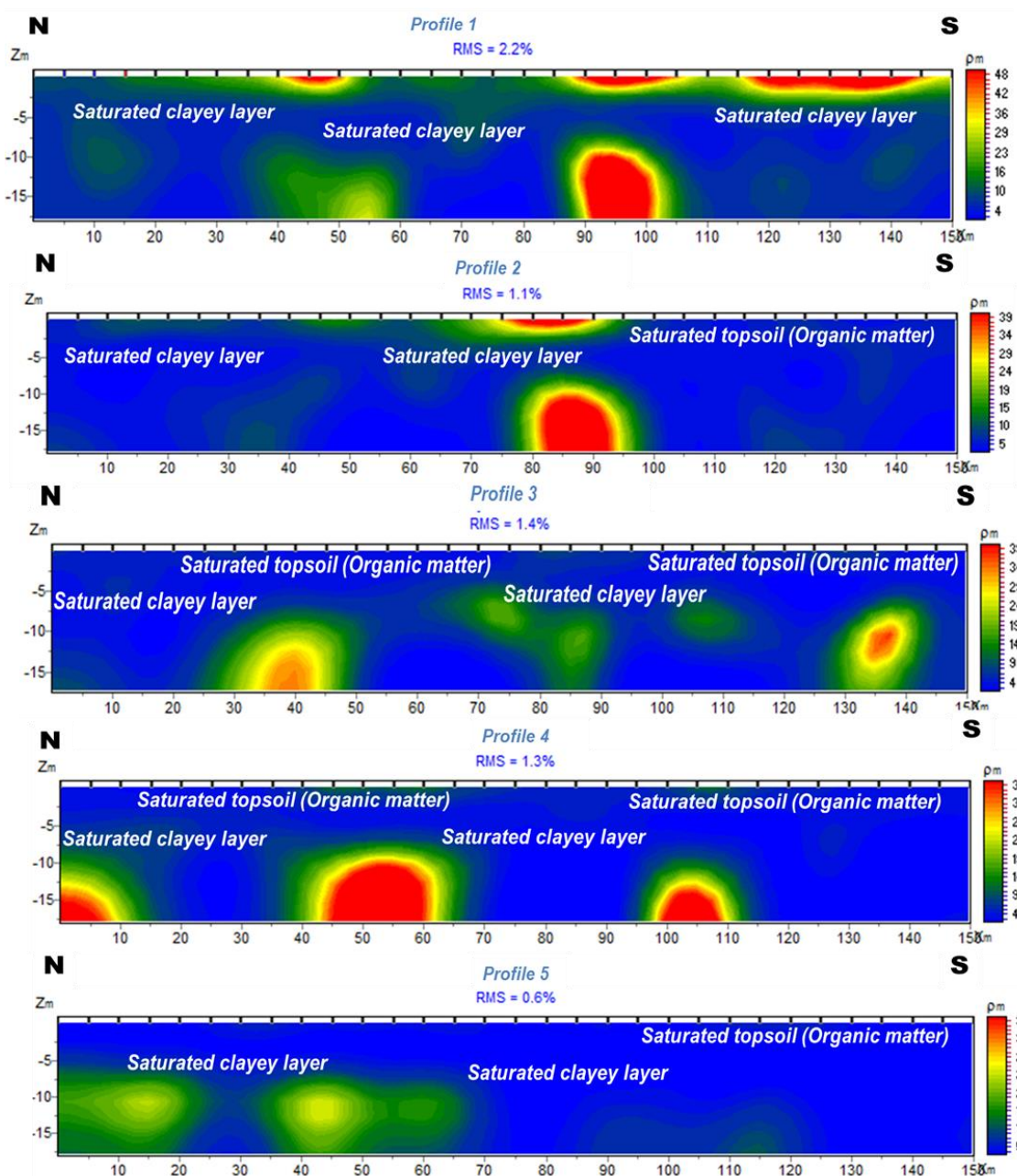


Figure 7a. Variation in the resistivity contours in the north-south direction

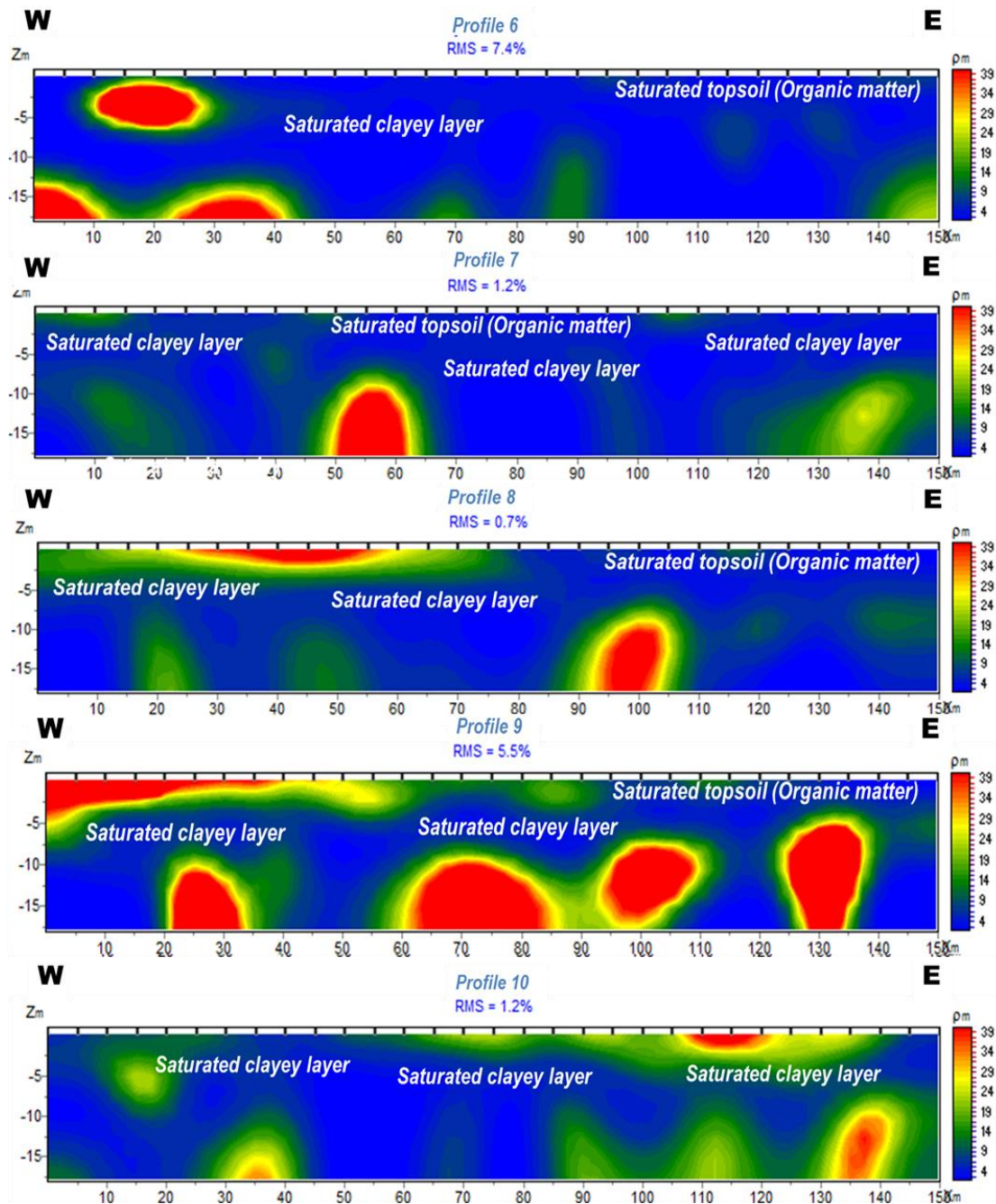


Figure 7b. Variation in the resistivity contours in the north-south direction

The variation in the subsurface resistivity at different depth is revealed in the combined inverted resistivity data generated as 2D along the X-Y direction. The resistivity depth map (Fig. 8) presents a better reflection of the subsurface geology in the study area and it showed resistivity variations at different depths in the study area. The 2D geo-resistivity map showed resistivity variations at different depths from the surface to a depth of about 30 m in the subsurface. It can be observed from the resistivity depth map that at the near surface it was characterized by saturated loamy clay, organic matter and organic peat which have almost the same resistivity value as saturated clayey formation. Therefore, the resistivity depth map presents both the near surface layer and the underlying layer

of saturated clayey formation as the same layer. The saturated alluvium occurs as pockets at the surface but at depth it increases in size. Fig. 9 presents the resistivity distribution for the study area along three orthogonal directions of X, Y and Z as a three-dimensional subsurface depth resistivity distribution model. This 3D model was generated from combination of the ten inverted 2D profiles occupied in north-south and west-east directions. This 3D model presents variations in subsurface resistivity across the study area at different depths to about 30 m below the surface. The 3D model displayed low resistivity layer at the surface with a pocket of high resistivity formation across the area. The high resistivity layer that appeared as a pocket at the surface increases in size with depth, while the low resistivity layer decreases in size with depth. The low resistivity layer is characterized by resistivity value of less than 10 Ωm to about 36 Ωm , which was interpreted as loamy clay, organic matter and peat at the surface and underlying by saturated clayey formation which has almost the same resistivity as the top layer. The presence of the loamy clay, organic matter, organic peat and clayey formation aided water retention within the subsurface, which were being made use of during dry season for food crop farming within the flood plain. The relatively high resistivity value was interpreted as alluvium. The observed variations in resistivity with depth, which distinguished both resistive and less resistive zones across the investigated area, further confirm the variations in the ground physical parameters along the three directions (X, Y and Z).

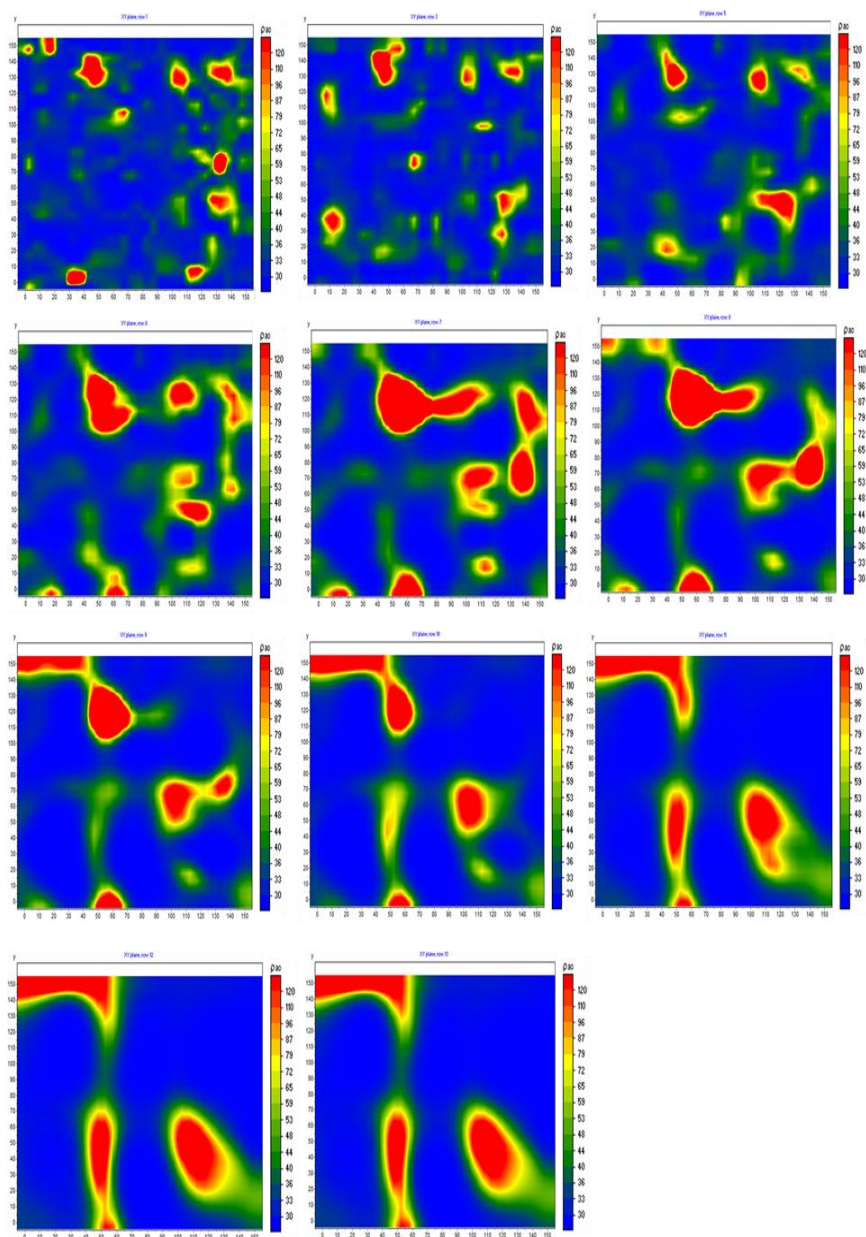


Figure 8. Combined inverted resistivity data generated as 2D along the X-Y direction

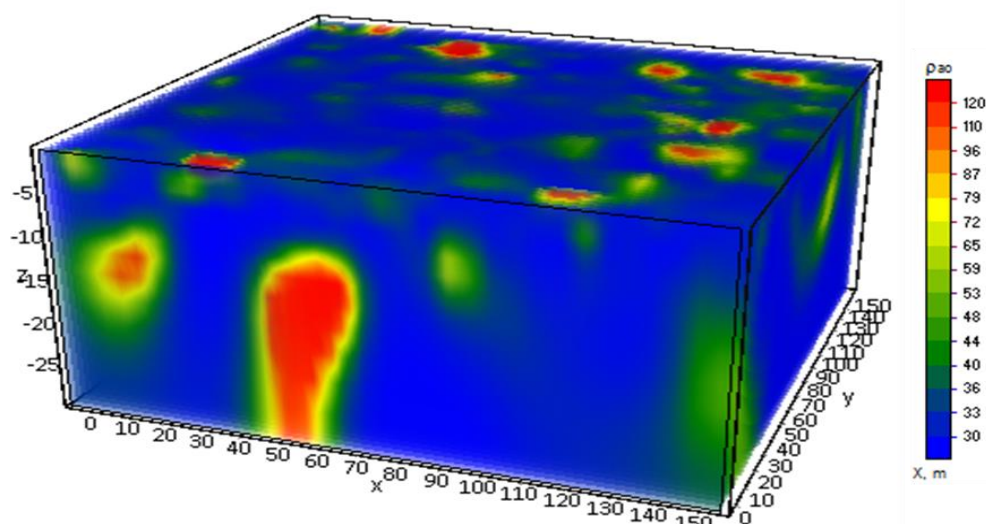


Figure 9. Resistivity distribution for the study area along three orthogonal directions of X, Y and Z as a three-dimensional subsurface depth resistivity distribution model

4.3 Ground Penetrating Radar (GPR) results

The frequency of GPR antennas and the electrical properties of soils are limiting factors to radar signal resolution and depth of penetration [41]. It has been observed that at about 200–300 cm below the ground surface is the occurrence of most soil properties, which coincides with the soil-vegetation interface relationships [42]. Representatives of the processed radar sections are shown in Figs. 10a and 10b, which were in the north-south and west-east directions respectively. From the radar sections, three dissimilar reflecting surfaces were identified and selected based on the principles of radar stratigraphy proposed by [43]. The first layer (Horizon 1), which is above the red line on the section, was characterized with continuous parallel, sub-parallel and varying dip reflections with low amplitude which is an indication of fine muddy soil that is copious in organic matter, peats, remains of plants and clay. This layer was referred to as topsoil. The material constituent of this component is recognized to have low permeability [44]. This layer has approximate thickness of about 0.5 m across the profiles. Underlying this layer (i.e. the layer above yellow line or Horizon 2) is a unique and conspicuous layer in the entire radar sections which was described by low amplitude, weak/structureless in addition to continuous reflections which is an indication of signal attenuation. Observation on the signal reflection indicates that this layer is characterized with high moisture content which was considered to be saturated loamy clay soil with high amount of clay content. Any formation with this characteristic is considered to correspond with deposit of swamp and as such it is expected to be of a low permeability [44]. This particular layer exhibits this saturation all year round due to its low permeability feature that allows its ability for water retention for food crop farming within the floodplain in dry season. The thickness of this layer ranges from 0.8 m to 1.9 m. The high amplitude, chaotic and sub-parallel layer with moderately continuous reflection was found at the base of the radar sections which is labelled Horizon 3. These characteristics depict that of alluvium which is the last layer observed on the radar section. Water table was found at the depth of less than 1 m on the profiles. The strength of the water-table radar reflector depends on the contrast between the electrical properties of the unsaturated and saturated zones. The capillary fringe is more gradual because of the presence of smaller, more continuous pore space, and the water-table is less distinct on the graphic record. Also, the water-table reflection is less abrupt.

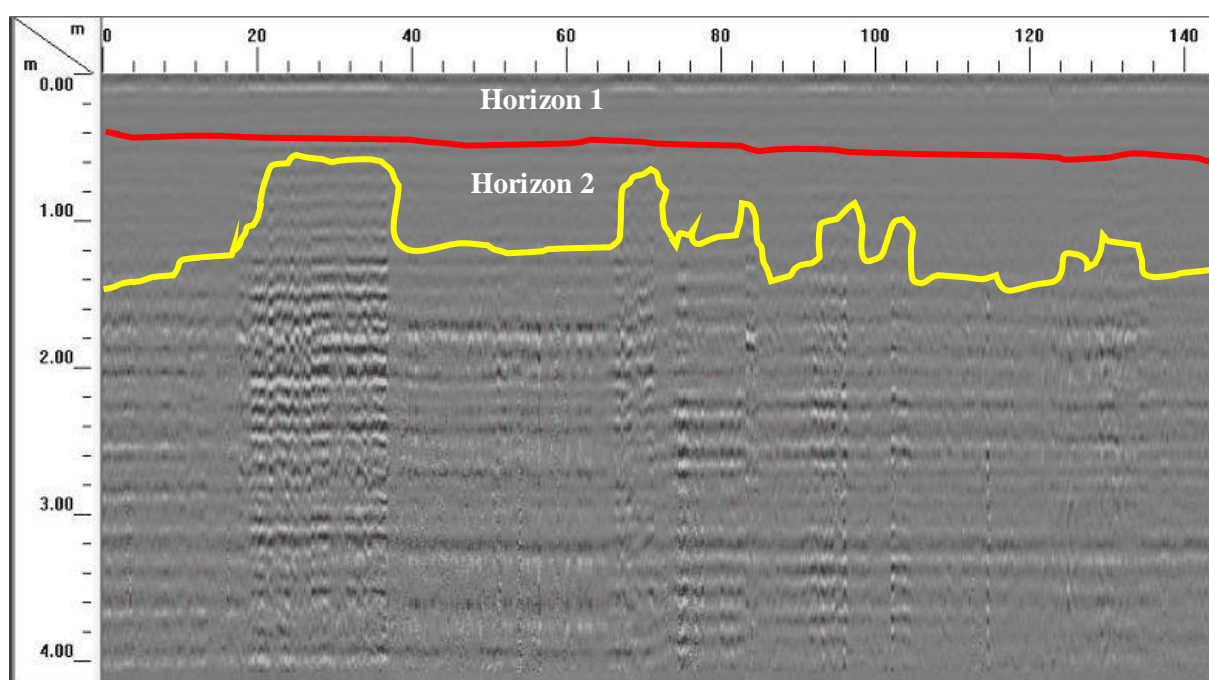


Figure 10a. Radar section along traverse line 5 along north-south direction using antenna frequency of 250 Hz

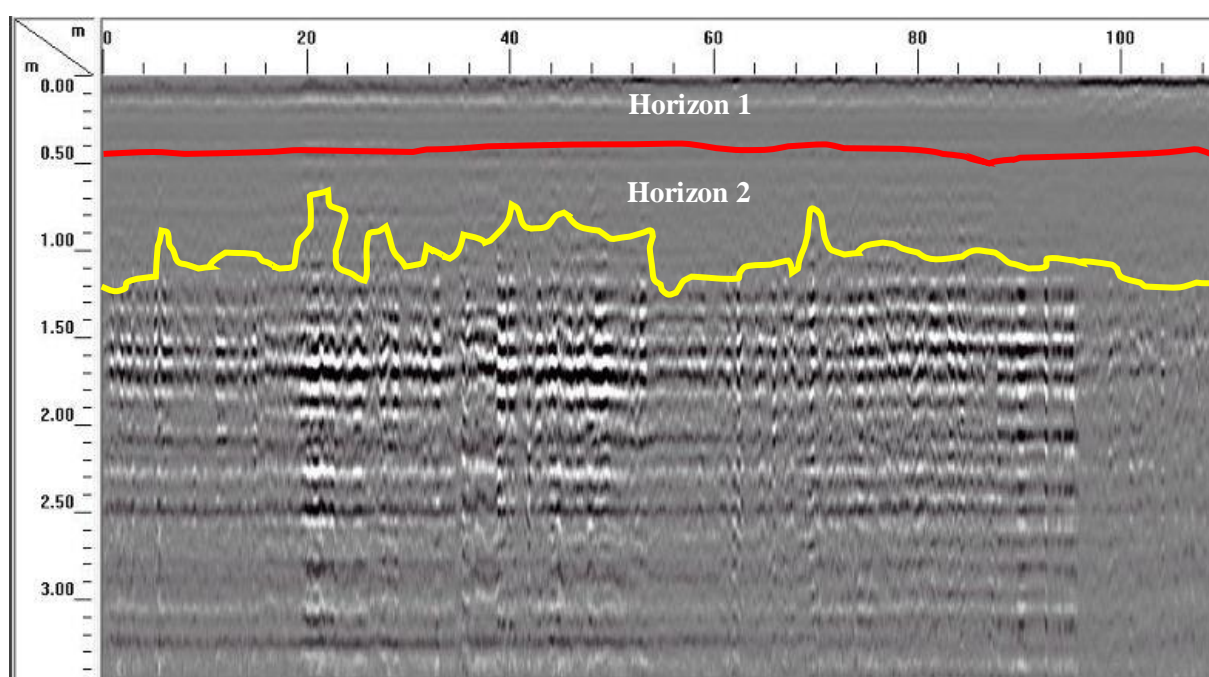


Figure 10b. Radar section along traverse line 7 along west- east direction using antenna frequency of 250 MHz

4.4 Correlation of Vertical Electrical Sounding (VES), Electrical Resistivity Imaging (ERI) and Ground Penetrating Radar (GPR)

The three geophysical methods used in this research work competently delineated three geologic layers. These are the topsoil, saturated loamy clay, and alluvium. Electrical resistivity results successfully mapped sequences of the lithology in the floodplain subsurface. Additionally, it provided an understanding of the materials that make up the three lithologic layers delineated. GPR results were able to delineate only the lithological sequences. It could not ascertain the structural details because the radar signal strength was low. This notwithstanding, the percentage of correlation of all the three geophysical methods used is high.

5 CONCLUSIONS

Integrated geophysical techniques involving Vertical Electrical Sounding (VES), Electrical Resistivity Imaging (ERI), and Ground Penetrating Radar (GPR) have been implemented in this study around Papalanto, Ogun River floodplain, Southwestern Nigeria. The results of the Electrical Resistivity (ER) investigation have effectively delineated the subsurface geological information and give a detailed description of the lithological setting within the area.

From the ER surveys, it was observed that the crops on the floodplain grow well during the dry season because it constitutes of the alluvium, being the most productive agricultural land. Depth to this proficient layer ranges from 3.1 to 37.4 m across the study area. This makes available adequate nutrients and water to the growing vegetables/crops with a shallow root system. The floodplain subsurface is also largely made up of clayey soils which have moisture and nutrient retention abilities that make the crop grow well. The study location can therefore be considered to have semi-competent to competent fertile agricultural land considering the resistivity distribution of the floodplain subsurface. Thus, electrical resistivity methods and ground-penetrating radar are versatile tools in shallow site characterization and should therefore be incorporated in any geophysical investigation for a better understanding of the subsurface geology.

REFERENCES

- [1] OPPERMAN, J.J., R. LUSTER, B.A. MCKENNY, M. ROBERTS and A.W. MEADOWS. Ecologically Functional Floodplains: Connectivity, Flow Regime, and Scale 1. *Journal of the American Water Resources Association*. 2010, vol. 46(2), pp. 211–226. ISSN 1752-1688. DOI: [10.1111/j.1752-1688.2010.00426.x](https://doi.org/10.1111/j.1752-1688.2010.00426.x)
- [2] MUTERT, E. Suitability of Soils for Oil Palm in Southeast Asia. *Better Crops International*. 1999, vol. 13(1), pp. 36–38. Available from: <http://www.ipni.net/publication/bci.nsf/issue/BC-INT-1999-1>
- [3] BASSO, L.R., A. BARTISS, Y. MAO, C.E. GAST, P.S.R. COELHO, M. SNYDER and B. WONG. Transformation of *Candida albicans* with a synthetic hygromycin B resistance gene. *Yeast*. 2010, vol. 27(12), pp. 1039–1048. ISSN 1097-0061. DOI: [10.1002/yea.1813](https://doi.org/10.1002/yea.1813)
- [4] MOSTAFA M., M.B. ANWAR and A. RADWAN. Application of electrical resistivity measurement as quality control test for calcareous soil. *HBRC Journal*. 2018, vol. 14(3), pp. 379–384. ISSN 1687-4048. DOI: [10.1016/j.hbrcj.2017.07.001](https://doi.org/10.1016/j.hbrcj.2017.07.001)
- [5] ABDEL AAL, G.Z., E.A. ATEKWANA, L.D. SLATER and C. ULRICH. Induced Polarization (IP) Measurements of Soils from an Aged Hydrocarbon Contaminated Site. In: *17th EEGS Symposium on the Application of Geophysics to Engineering and Environmental Problems Proceedings: February 22–26, 2004, Colorado Springs, Colorado, USA*. Environmental & Engineering Geophysical Society, 2004, pp. 190–201. ISSN 1554-8015. DOI: [10.4133/1.2923160](https://doi.org/10.4133/1.2923160)
- [6] DOSER, D.I., O.S. DENA-ORNELAS, R.P. LANGFORD and M.R. BAKER. Monitoring Yearly Changes and Their Influence on Electrical Properties of the Shallow Subsurface at Two Sites Near the Rio Grande, West Texas. *Journal of Environmental & Engineering Geophysics*. 2004, vol. 9(4), pp. 179–226. ISSN 1083-1363. DOI: [10.4133/JEEG9.4.179](https://doi.org/10.4133/JEEG9.4.179)
- [7] SUDHA, K., M. ISRAIL, S. MITTAL and J. RAI. Soil characterization using electrical resistivity tomography and geotechnical investigations. *Journal of Applied Geophysics*. 2009, vol. 67(1), pp. 74–79. ISSN 0926-9851. DOI: [10.1016/j.jappgeo.2008.09.012](https://doi.org/10.1016/j.jappgeo.2008.09.012)

- [8] AIZEBEOKHAI, A.P. and K.D. OYEYEMI. The use of the multiple-gradient array for geoelectrical resistivity and induced polarization imaging. *Journal of Applied Geophysics*. 2014, vol. 111, pp. 364–376. ISSN 0926-9851. DOI: [10.1016/j.jappgeo.2014.10.023](https://doi.org/10.1016/j.jappgeo.2014.10.023)
- [9] DAFALLA, M.A. and F.A. ALFOUZAN. Influence of Physical Parameters and Soil Chemical Composition on Electrical Resistivity: A Guide for Geotechnical Soil Profiles. *International Journal of Electrochemical Science*. 2012, vol. 7(4), pp. 3191–3204. ISSN 1452-3981. Available from: <http://www.electrochemsci.org/papers/vol7/7043191.pdf>
- [10] MICHOT, D., Y. BENDERITTER, A. DORIGNY, B. NICOUILLAUD, D. KING and A. TABBAGH. Spatial and temporal monitoring of soil water content with an irrigated corn crop cover using surface electrical resistivity tomography. *Water Resources Research*. 2003, vol. 39(5). ISSN 1944-7973. DOI: [10.1029/2002WR001581](https://doi.org/10.1029/2002WR001581)
- [11] SAMOUËLIAN, A., I. COUSIN, A. TABBAGH, A. BRUAND and G. RICHARD. Electrical resistivity survey in soil science: a review. *Soil and Tillage Research*. 2005, vol. 83(2), pp. 173–193. ISSN 0167-1987. DOI: [10.1016/j.still.2004.10.004](https://doi.org/10.1016/j.still.2004.10.004)
- [12] ROSSI, R., M. AMATO, G. BITELLA, R. BOCHICCHIO, J.J. FERREIRA GOMEZ, S. LOVELLI, E. MARTORELLA and P. FAVALE. Electrical resistivity tomography as a non-destructive method for mapping root biomass in an orchard. *European Journal of Soil Science*. 2011, vol. 62(2), pp. 206–215. ISSN 1365-2389. DOI: [10.1111/j.1365-2389.2010.01329.x](https://doi.org/10.1111/j.1365-2389.2010.01329.x)
- [13] ABIDIN, M.H.Z., F. AHMAD, D.C. WIJESEKERA, R. SAAD and M.F.T. BAHARUDDIN. Soil Resistivity Measurements to Predict Moisture Content and Density in Loose and Dense Soil. *Applied Mechanics and Materials*. 2013, vols. 353–356, pp. 911–917. ISSN 1662-7482. DOI: [10.4028/www.scientific.net/AMM.353-356.911](https://doi.org/10.4028/www.scientific.net/AMM.353-356.911)
- [14] BHATT, S. and P.K. JAIN. Correlation between electrical resistivity and water content of sand – a statistical approach. *American International Journal of Research in Science, Technology, Engineering & Mathematics*. 2014, vol. 6(2), pp. 115–121. ISSN 2328-3491. Available from: <http://iasir.net/AIJRSTEMpapers/AIJRSTEM14-342.pdf>
- [15] NOVÁKOVÁ, E., M. KAROUS, A. ZAJÍČEK, and M. KAROUSOVA. Evaluation of ground penetrating radar and vertical electrical sounding methods to determine soil horizons and bedrock at the locality Dehtáře. *Soil and Water Research*. 2013, vol. 8(3), pp. 105–112. ISSN 1801-5395. DOI: [10.17221/6/2012-SWR](https://doi.org/10.17221/6/2012-SWR)
- [16] GARCIA-MONTIEL, D.C., M.T. COE, M.P. CRUZ, J.N. FERREIRA, E.M. DA SILVA and E.A. DAVIDSON. Estimating seasonal charges in volumetric soil water content at landscape scales in a savanna ecosystem using two-dimensional resistivity profiling. *Earth Interact.* 2008, vol. 12(2), pp. 1–25. ISSN 1087-3562. DOI: [10.1175/2007EI238.1](https://doi.org/10.1175/2007EI238.1)
- [17] GOLEKAR, R.B., M.V. BARIDE and S.N. PATIL. 1D resistivity sounding geophysical survey by using Schlumberger electrode configuration method for groundwater exploration in catchment area of Anjani and Jhiri river, Northern Maharashtra (India). *Journal of Spatial Hydrology*. 2014, vol. 12(1), pp. 22–36. ISSN 2572-4479. Available from: <https://scholarsarchive.byu.edu/josh/vol12/iss1/1/>
- [18] MICHOT, D., Y. BENDERITTER, A. DORIGNY, B. NICOUILLAUD, D. KING and A. TABBAGH. Spatial and temporal monitoring of soil water content with an irrigated corn crop covers using electrical resistivity tomography. *Water Resources Research*. 2003, vol. 39(5). ISSN 1944-7973. DOI: [10.1029/2002WR001581](https://doi.org/10.1029/2002WR001581)
- [19] BESSON, A., I. COUSIN, A. SAMOUËLIAN, H. BOIZARD and G. RICHARD. Structural heterogeneity of the soil tilled layers as characterized by 2D electrical resistivity surveying. *Soil and Tillage Research*. 2004, vol. 79(2), pp. 239–249. ISSN 0167-1987. DOI: [10.1016/j.still.2004.07.012](https://doi.org/10.1016/j.still.2004.07.012)
- [20] MOKMA, D.L., R.J. SCHAEZL, J.A. DOOLITTLE and E.P. JOHNSON. Ground-penetrating radar study of Ortstein continuity in some Michigan haplaquods. *Soil Science Society of America Journal*. 1990, vol. 54(3), pp. 936–938. ISSN 1435-0661. DOI: [10.2136/sssaj1990.03615995005400030056x](https://doi.org/10.2136/sssaj1990.03615995005400030056x)
- [21] POOLE, F.G., W.R. PAGE and R. AMAYA-MARTÍNEZ. Newly discovered Silurian carbonate-shelf rocks in west-central Sonora, Mexico. *Geological Society of America: Abstracts with Programs*. 1997, vol. 29(6), p. 483.
- [22] CONYERS, L.B. and D. GOODMAN. *Ground-Penetrating Radar: An Introduction for Archaeologists*. Walnut Creek (CA): Alta Mira Press, 1997. ISBN 9780761989288.
- [23] MELLET, J.S. Ground penetrating radar applications in engineering, environmental management, and geology. *Journal of Applied Geophysics*. 1995, vol. 33(1–3), pp. 157–166. ISSN 0926-9851. DOI: [10.1016/0926-9851\(95\)90038-1](https://doi.org/10.1016/0926-9851(95)90038-1)
- [24] JOL, H.M. (ed.). *Ground Penetrating Radar: Theory and Applications*. Elsevier Science Ltd, 2009. eBook ISBN: 9780080951843.
- [25] ONAKOMAIYA, S.O. et al. *Ogun State in Maps*. Ibadan: Rex Charles Publication, 1992. ISBN 9789782137364.

- [26] NIGERIA GEOLOGICAL SURVEY AGENCY. *The Geological Map of Nigeria*. Abuja (Nigeria): N.G.S.A, 2009.
- [27] ADEGOKE, O.S., A.E. AGUMANU, M.J. BENKHELIL and P.O. AJAYI. New stratigraphic sedimentologic and structural data on the Kerri-Kerri Formation, Bauchi and Bornu States, Nigeria. *Journal of African Earth Sciences*. 1986, vol. 5(3), pp. 249–277. ISSN 0731-7247. DOI: [10.1016/0899-5362\(86\)90016-3](https://doi.org/10.1016/0899-5362(86)90016-3)
- [28] LONGE, E.O., S. MALOMO and M.A. OLORUNNIWO. Hydrogeology of Lagos metropolis. *Journal of African Earth Sciences*. 1987, vol. 6(2), pp. 163–174. ISSN 0731-7247. DOI: [10.1016/0899-5362\(87\)90058-3](https://doi.org/10.1016/0899-5362(87)90058-3)
- [29] OKE, S.A. Regional Aquifer Vulnerability and Pollution Sensitivity Analysis of Drastic Application to Dahomey Basin of Nigeria. *International Journal of Environmental Research and Public Health*. 2020, vol. 17(7), art. no. 2609. ISSN 1660-4601. DOI: [10.3390/ijerph17072609](https://doi.org/10.3390/ijerph17072609)
- [30] GEBHARDT, H., O.A. ADEKEYE and S.O. AKANDE. Late Paleocene to initial Eocene Thermal Maximum (IETM) Foraminiferal Biostratigraphy and Paleocology of the Dahomey Basin, Southwestern Nigeria. *Jahrbuch der Geologischen Bundesanstalt*. 2010, vol. 150(3+4), pp. 407–419. ISSN 0016–7800. Available from: https://www.zobodat.at/pdf/JbGeolReichsanst_150_0407-0419.pdf
- [31] BIAŁOSTOCKI, R. and J. FARBISZ. Badania geoelektryczne – elektrooporowe. Stan aktualny i możliwości wykorzystania wyników. *Geofizyka: Biuletyn Informacyjny*. 2007, vol. 5, pp. 28–41.
- [32] FARBISZ, J., R. BIAŁOSTOCKI and K. ZOCHNIAK. Badania geoelektryczne-elektrooporowe w PBG – wczoraj, dziś i w perspektywie najbliższych lat. *Geofizyka: Biuletyn Informacyjny*. 2010, vol. 8, pp. 86–107.
- [33] LOKE, M.H. and R.D. BARKER. Rapid least-squares inversion of apparent resistivity pseudosections by a quasi-Newton method. *Geophysical Prospecting*. 1996, vol. 44(1), pp. 131–152. ISSN 1365-2478. DOI: [10.1111/j.1365-2478.1996.tb00142.x](https://doi.org/10.1111/j.1365-2478.1996.tb00142.x)
- [34] LOKE, M.H., I. ACWORTH and T. DAHLIN. A comparison of smooth and blocky inversion methods in 2D electrical imaging surveys. *Exploration Geophysics*. 2003, vol. 34(3), pp. 182–187. ISSN 0812-3985. DOI: [10.1071/EG03182](https://doi.org/10.1071/EG03182)
- [35] BEST, J., J. WOODWARD, P. ASHWORTH, G.S. SMITH and C. SIMPSON. Bar-top hollows: A new element in the architecture of sandy braided rivers. *Sedimentary Geology*. 2006, vol. 190(1–4), pp. 241–255. ISSN 0037-0738. DOI: [10.1016/j.sedgeo.2006.05.022](https://doi.org/10.1016/j.sedgeo.2006.05.022)
- [36] CASSIDY, N.J. Chapter 5 – Ground Penetrating Radar Data Processing, Modelling and Analysis. In: JOL, H.M. (ed.). *Ground Penetrating Radar: Theory and Applications*. Amsterdam, Elsevier Science, 2009, pp. 141–176. ISBN 978-0-444-53348-7. DOI: [10.1016/B978-0-444-53348-7.00005-3](https://doi.org/10.1016/B978-0-444-53348-7.00005-3)
- [37] MITCHUM, R.M., P.R. VAIL and J.B. SANGREE. Seismic Stratigraphy and Global Changes of Sea Level, Part 6: Stratigraphic Interpretation of Seismic Reflection Patterns in Depositional Sequences. In: PAYTON, C.E. (ed.). *Seismic Stratigraphy – Applications to Hydrocarbon Exploration*. AAPG, 1977, pp. 117–133. ISBN 9781629812052. DOI: [10.1306/M26490C8](https://doi.org/10.1306/M26490C8)
- [38] JONES, M. J. The weathered zone aquifers of the basement complex areas of Africa. *Quarterly Journal of Engineering Geology and Hydrogeology*. 1985, vol. 18(1), pp. 35–46. ISSN 1470-9236. DOI: [10.1144/GSL.QJEG.1985.018.01.06](https://doi.org/10.1144/GSL.QJEG.1985.018.01.06)
- [39] TELFORD, W.M., L.P. GELDART and R.E. SHERIFF. Chapter 8 – Resistivity Methods. In: *Applied Geophysics*. 2nd edition. Cambridge (UK): Cambridge University Press, 1991, pp. 522–577. ISBN 9780521339384. DOI: [10.1017/CBO9781139167932.012](https://doi.org/10.1017/CBO9781139167932.012)
- [40] MCGINNIS, L.D. and T.E. JENSEN. Permafrost – hydrogeologic regimen in two ice-free valleys, Antarctica, from electrical depth sounding. *Quaternary Research*. 1971, vol. 1(3), pp. 389–409. ISSN 0033-5894. DOI: [10.1016/0033-5894\(71\)90073-1](https://doi.org/10.1016/0033-5894(71)90073-1)
- [41] DOOLITTLE, J.A. and J.R. BUTNOR. Chapter 6 – Soils, Peatlands, and Biomonitoring. In: JOL, H.M. (ed.). *Ground Penetrating Radar: Theory and Applications*. Amsterdam, Elsevier Science, 2009, pp.178–202. ISBN 978-0-444-53348-7. DOI: [10.1016/B978-0-444-53348-7.00006-5](https://doi.org/10.1016/B978-0-444-53348-7.00006-5)
- [42] DE MENDONÇA, B.A.F., E.I. FERNANDES FILHO, C.E.G.R. SCHAEFER, A.F. DE CARVALHO, J.F. DO VALE JR. and G.R. CORRÊA. Use of geophysical methods for the study of sandy soils under Campinarana at the National Park of Viruá, Roraima state, Brazilian Amazonia. *Journal of Soils and Sediments*. 2014, vol. 14, pp. 525–537. ISSN 1439-0108. DOI: [10.1007/s11368-013-0811-2](https://doi.org/10.1007/s11368-013-0811-2)
- [43] BERES, M. and F.P. HAENI. Application of Ground-Penetrating-Radar Methods in Hydrogeology Studies. *Groundwater*. 1991, vol. 29 (3), pp. 375–386. ISSN 1745-6584. DOI: [10.1111/j.1745-6584.1991.tb00528.x](https://doi.org/10.1111/j.1745-6584.1991.tb00528.x)
- [44] DARA, R., N. KETTRIDGE, M.O. RIVETT, S. KRAUSE and D. GOMEZ-ORTIZ. Identification of floodplain and riverbed sediment heterogeneity in a meandering UK lowland stream by ground penetrating radar. *Journal of Applied Geophysics*. 2019, vol. 171, art. no. 103863. ISSN 0926-9851. DOI: [10.1016/j.jappgeo.2019.103863](https://doi.org/10.1016/j.jappgeo.2019.103863)